

Prototypical Contrast and Reverse Prediction: Unsupervised Skeleton Based Action Recognition

Shihao Xu, Haocong Rao, Xiping Hu, Bin Hu

Abstract—In this paper, we focus on unsupervised representation learning for skeleton-based action recognition. Existing approaches usually learn action representations by sequential prediction but they suffer from the inability to fully learn semantic information. To address this limitation, we propose a novel framework named Prototypical Contrast and Reverse Prediction (PCR-P), which not only creates reverse sequential prediction to learn low-level information (*e.g.*, body posture at every frame) and high-level pattern (*e.g.*, motion order), but also devises action prototypes to implicitly encode semantic similarity shared among sequences. In general, we regard action prototypes as latent variables and formulate PCR-P as an expectation-maximization task. Specifically, PCR-P iteratively runs (1) E-step as determining the distribution of prototypes by clustering action encoding from the encoder, and (2) M-step as optimizing the encoder by minimizing the proposed ProtoMAE loss, which helps simultaneously pull the action encoding closer to its assigned prototype and perform reverse prediction task. Extensive experiments on N-UCLA, NTU 60, and NTU 120 dataset present that PCR-P outperforms state-of-the-art unsupervised methods and even achieves superior performance over some of supervised methods. Codes are available at <https://github.com/Mikexu007/PCR-P>.

I. INTRODUCTION

As an essential branch in computer vision, skeleton based action recognition has drawn broad attention due to the compact and effective skeletal representation of human body and its robustness against viewpoint variations and noisy backgrounds [5], [19], [32], [33].

Many of current skeleton-based works [5], [40], [42] for action recognition resort to supervised learning paradigms to learn action representations, which require massive annotated samples for training. However, the annotated information sometimes is not available or demand expensive labor force for labelling, which might face uncertain labelling or mislabelling challenges due to the high inter-class similarity of actions [7], [38]. From this perspective, exploiting the unlabeled data to learn effective action representations arouses considerable interests [15], [24].

In recent years, a stream of unsupervised learning methods have been introduced. Most of them [20], [22], [29], [34], [44] are built upon encoder-decoder structures [1] to yield discriminative action representations via sequential prediction/reconstruction or augmented sequence contrast. However, these methods suffer from a common significant disadvantage: Higher-level semantics (*e.g.*, motion order, semantic similarity among sequences) is not fully explored. This issue derives from the instance-level situation that the sequential prediction task forces the predicted sequence to get closer to only the

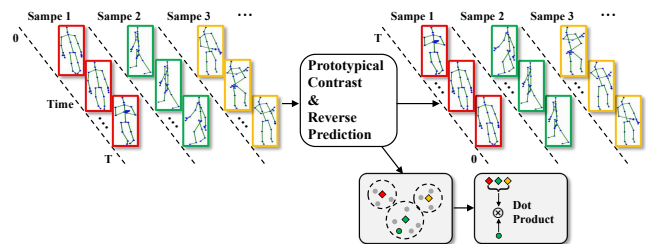


Fig. 1. Illustration of Prototypical Contrast and Reverse Prediction framework.

original one, but neglect the semantic similarity between various instances. Likewise, augmented sequence contrast is also restricted in pulling closer two augmented samples of one sequence regardless of others. Furthermore, this problem is worsened in large-scale datasets, since the correlation shared among numerous semantically similar samples cannot be fully exploited.

To address the challenges above, we rethink the encoder-decoder based sequential prediction in terms of expectation-maximization (EM) algorithm [6], and propose Prototypical Contrast and Reverse Prediction (PCR-P) framework. Fig. 1 illustrates the proposed PCR-P. An action prototype, similar to an image prototype [18], is a representative encoding for a bunch of semantically similar sequences. Instead of directly using encoder-decoder structure to obtain representation via data prediction, we exploit the EM algorithm to encode semantic structure of data into action representations by (1) implicitly learning semantic similarity between sequences to force the action encoding to approach their corresponding prototypes, and (2) learning high-level information (*e.g.*, motion order) of sequences via predicting sequence in reverse order.

Specifically, we focus on the encoder parameter learning in the EM algorithm and regard action prototypes as additional latent variables. From this perspective, the EM algorithm attempts to find a maximum likelihood estimate of encoder parameters (see Fig. 2(a)), while the decoder keeps fixed for enhancing the encoder to learn representations [34]. Given the current encoder parameters, the expectation step (E-step) aims to estimate the probability of prototypes by performing *k*-means clustering on the action encoding (the output at final step) from the Uni-GRU encoder, and the maximization step (M-step) tries to update the encoder parameters by minimizing the proposed loss, namely, ProtoMAE (Sec. IV-B2). Minimizing ProtoMAE is equivalent to maximizing the estimated likelihood under the assumption that the distribution around each prototype is isotropic Gaussian [18]. It is also equivalent to help predict sequence reversely and simultaneously pull

the action encoding closer to its corresponding prototype compared to other prototypes (see Fig. 2(b)). The E-step and the M-step function iteratively. In this way, the encoder is able to learn discriminative action representations without labeled data, and after convergence, it can be used for other downstream tasks such as classification. The contributions of our work are listed as follows:

- We propose a novel framework named Prototypical Contrast and Reverse Prediction to explore high-level information of sequences and that of the global dataset. To our knowledge, this work is the first to introduce prototypical contrast and reverse prediction for unsupervised skeleton based action recognition.
- We formulate the PCRPs into an EM iteration manner, in which the alternating steps of clustering and reverse prediction serve to approximate and maximize the log-likelihood function.
- We introduce ProtoMAE, an enhanced MAE loss that exploits contrastive loss to achieve high-level information learning as well as to adaptively estimate the tightness of the feature distribution around each prototype.
- Experiments on the N-UCLA, NTU RGB+D 60, and NTU RGB+D 120 dataset, show the superiority of our framework to other state-of-the-art unsupervised methods as well as some of supervised counterparts.

II. RELATED WORK

Unsupervised action Recognition: While supervised methods [5], [19], [31] show great performance in skeleton based action recognition by using annotated information, *unsupervised* methods are advantageous at learning action representation without any labels. Zheng *et al.* [44] introduce a generative adversarial network (GAN) based encoder-decoder for skeletal sequence regeneration, and utilize the representation learned from encoders to identify actions. Su *et al.* [34] further devise predict&cluster (P&C) model with decoder-weakening mechanism to enhance the ability of the encoder to capture more discriminative action pattern. Rao *et al.* [29] propose skeleton augmentation strategies and apply momentum LSTM with contrastive learning to learn robust action representation. However, these methods ignore the semantic information between different sequences. In this paper, we adopt encoder-decoder structure with decoder-weakening strategy [34] as the backbone, and propose prototypical contrast for semantic learning and achieve sequential reverse prediction for enhancing representation learning.

Unsupervised Action Clustering: Many clustering based models have been introduced for unsupervised action clustering. Jones *et al.* [14] propose dual assignment k-means (DAKM) to achieve context learning for facilitating unsupervised action clustering. Bhatnagar *et al.* [2] devise weak learner based autoencoders to extract temporal features under different temporal resolutions. Peng *et al.* [28] establish a recursive constrained model by using the contextual motion and scene for unsupervised video action clustering. Nevertheless, these approaches only serve for RGB videos and yet the counterpart for skeleton action sequences is not developed.

In this proposed work, we for the first time explore the prototypical contrast for unsupervised skeleton based action recognition.

Contrastive Learning: In recent years, contrastive learning, a type of unsupervised (self-supervised) learning method, has attracted massive attention. Most of them [3], [4], [12], [18] learn effective representations by pretext tasks [39], [45] with contrastive losses [10], [11]. For example, Wu *et al.* [39] base an instance contrast task and noise-contrastive estimation (NCE) loss [10] to match positive pairs and push apart negative pairs. He *et al.* [12] propose momentum based encoder to learn more consistent representations. Nevertheless, these methods mainly focus on image representation learning. In this paper, we introduce prototypical contrast [18] to skeleton based action recognition and improve the sequential prediction task on high-level semantics learning.

III. PRELIMINARIES

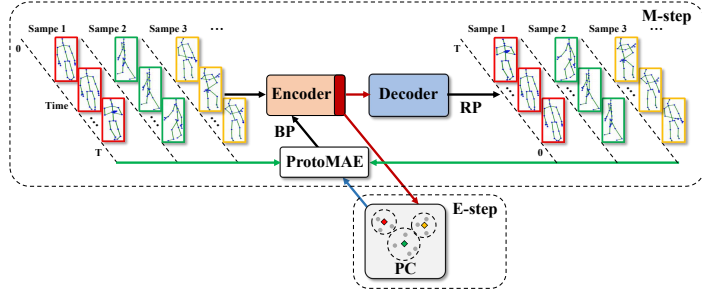
We focus on the unsupervised representation learning using skeleton sequences. Then, we exploit the learned representations for skeleton-based action recognition. Given a training set $\Phi = \{\mathbf{x}^{(i)}\}_{i=1}^N$ of N skeleton sequences, each sequence $\mathbf{x} \in \mathbb{R}^{T \times J \times 3}$ contains T skeleton frames and each frame has J body joints that are represented in 3D space. Our goal is to learn an encoder f_E (we employ Uni-GRU) that maps Φ to action encoding set $V = \{\mathbf{v}^{(i)}\}_{i=1}^N$, where $\mathbf{v}^{(i)} \in \mathbb{R}^C$ is a discriminative action representation of $\mathbf{x}^{(i)}$. Traditional encoder-decoder based models achieve this goal by sequential prediction as to optimize the loss function of mean square error (MSE) or mean absolute error (MAE) between the original sequence and its predicted one. MAE/MSE only focus on skeleton reconstruction within each single sequence and ignore the similarity of different sequences. In our proposed framework PCRPs, we tackle this challenge by introducing action prototypical contrast paradigm (see Sec. IV-A1). Besides, we achieve sequential prediction in reverse order (see Sec. IV-B1) to enhance high-level information (*e.g.*, motion pattern) learning. Fig. 2(a) illustrates our framework, where semantic learning and data reverse prediction are performed alternately at each epoch. The main algorithm of PCRPs is shown in Algorithm 1.

Before introducing our proposed PCRPs, we first have a brief review of the general encoder-decoder based sequential prediction task that we rely on.

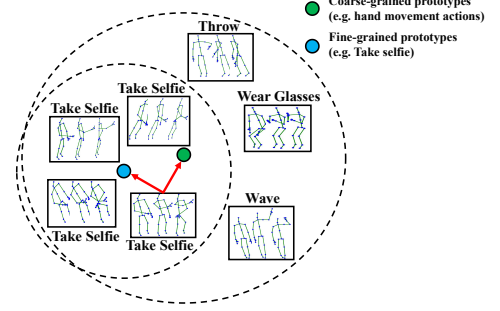
A. Sequential Prediction

Given a skeleton sequence $\mathbf{x} = \{\mathbf{x}_1, \dots, \mathbf{x}_T\}$, the model is expected to output the predicted sequence $\hat{\mathbf{x}} = (\hat{\mathbf{x}}_1, \dots, \hat{\mathbf{x}}_T)$ that gets closer as much as possible to \mathbf{x} . In training phase, the encoder (*e.g.*, Uni-GRU) encodes every skeleton frame \mathbf{x}_t ($t \in \{1, \dots, T\}$) and the previous step's latent state \mathbf{h}_{t-1} ($t-1 > 0$) to determine the current output \mathbf{v}_t and the current latent state \mathbf{h}_t :

$$(\mathbf{v}_t, \mathbf{h}_t) = \begin{cases} f_E(\mathbf{x}_t) & \text{if } t = 1 \\ f_E(\mathbf{h}_{t-1}, \mathbf{x}_t) & \text{if } t > 1 \end{cases} \quad (1)$$



(a) Illustration of PCR in view of EM algorithm. In E-step, the action encoding from the final output of the encoder is used for clustering. In M-step, the action encoding is fed into the decoder for predicting sequence reversely, and ProtoMAE loss is minimized to update the encoder. BP denotes back propagation.



(b) An action encoding can be assigned to different action prototypes with different granularity. PCR attempts to pull the encoding closer to the most suitable prototype.

Fig. 2.

Algorithm 1 Main algorithm of PCR

Input: encoder f_E , decoder f_D , training dataset Φ , number of clusters $K = \{k_m\}_{m=1}^M$

while not MaxEpoch **do**

 # E-step

$V = f_E(\Phi)$ # obtain action encoding for all training data

for $m = 1$ **to** M **do**

 # cluster V into k_m clusters and return prototypes.

$Z^m = k\text{-means}(V, k_m)$

 # calculate the distribution tightness of each prototype with Eq. 8

$\phi_m = \text{Tightness}(Z^m, V)$

end for

 # M-step

for a mini-batch x in Φ **do**

$v = f_E(x)$

$\hat{x} = f_D(v)$

$\bar{x} = \text{Reverse}(x)$

 # compute loss with Eq.13

$\mathcal{L}_{\text{ProtoMAE}}(v, \bar{x}, \hat{x}, \{Z^m\}_{m=1}^M, \{\phi_m\}_{m=1}^M)$

 fix f_D # parameters of decoder do not evolve

 Update f_E to minimize $\mathcal{L}_{\text{ProtoMAE}}$ with Adam optimizer

end for

end while

where $v_t, h_t \in \mathbb{R}^C$. Next, the decoder f_D utilizes the output at final step v_T from the encoder to perform prediction task:

$$\left(\hat{x}_t, \hat{h}_t\right) = \begin{cases} f_D(v_T) & \text{if } t = 1 \\ f_D(\hat{h}_{t-1}) & \text{if } t > 1 \end{cases} \quad (2)$$

Then MAE loss is applied on x and \hat{x} for model optimization. Therefore, v_T is the action encoding (*i.e.*, representation) of the sequence x .

IV. PROTOTYPICAL CONTRAST AND REVERSE PREDICTION AS EXPECTATION-MAXIMIZATION

Sequence prediction based PCR aims to find the encoder parameters θ that maximizes the likelihood function of the N observed sequences:

$$\theta^* = \arg \max_{\theta} \sum_{i=1}^N \log p(x^{(i)} | \theta) \quad (3)$$

Since the action prototypes are introduced but not directly observed, they are viewed as the latent variables of observed

data given by $Z = \{z_i\}_{i=1}^K$ with K action prototypes, where $z_i \in \mathbb{R}^C$. Thus the Eq. 3 is referred to as:

$$\theta^* = \arg \max_{\theta} \sum_{i=1}^N \log \sum_{z_i \in Z} p(x^{(i)}, z_i | \theta). \quad (4)$$

Achieving this function directly is challenging, and the only knowledge of action prototypes Z is obtained in the posterior distribution $p(z_i | x^{(i)}, \theta)$. Under this circumstance, we first utilizes current parameters θ^{old} and the Jensen's inequality to turn Eq. 4 into an expectation¹ $\mathcal{Q}(\theta, \theta^{\text{old}})$ that needs to be maximized:

$$\theta^* = \arg \max_{\theta} \mathcal{Q}(\theta, \theta^{\text{old}}), \quad (5)$$

$$\mathcal{Q}(\theta, \theta^{\text{old}}) = \sum_{i=1}^N \sum_{z_i \in Z} p(z_i | x^{(i)}, \theta^{\text{old}}) \log p(x^{(i)}, z_i | \theta). \quad (6)$$

Then we rely on the EM algorithm with E-step and M-step to achieve Eq. 5.

A. E-step

In this step, we attempt to estimate $p(z_i | x^{(i)}, \theta^{\text{old}})$ of Eq. 6 and introduce prototypical contrast.

1) *Prototypical Contrast:* The result of $p(z_i | x^{(i)}, \theta^{\text{old}})$ is based on the action prototype z_i . Along this line, we take advantage of the action encoding from encoder to obtain z_i . Specifically, we apply k -means algorithm on all action encoding $\{v_T^{(i)}\}_{i=1}^N$ (the final output) from f_E to obtain K clusters, in which we define prototype $z_i \in \mathbb{R}^C$ as the centroid of the i^{th} cluster [18]. Therefore, we have

$$p(z_i | x^{(i)}, \theta^{\text{old}}) = \begin{cases} 0 & \text{if } v_T^{(i)} \notin z_i \\ 1 & \text{if } v_T^{(i)} \in z_i \end{cases}. \quad (7)$$

Using the action encoding from encoder to achieve prototypical contrast is beneficial due to several aspects: (1) The action encoding is in low dimension compared with the whole

¹More details are given in Supplementary Materials.

sequence. (2) The action encoding contains abundant context information of the action. (3) Semantic similarity between different samples is explored by pulling the action encoding closer to their corresponding prototypes (see Sec. IV-B2).

2) *Tightness Estimation*: To measure the cluster’s quality (feature distribution), we introduce the tightness $\phi \propto \sigma^2$ [18]. We first suppose a cluster has a prototype \mathbf{z}_i and contains P action encoding vectors $\left\{ \mathbf{v}_T^{(i)} \right\}_{i=1}^P$, which are then used to compute ϕ . Here a good ϕ is expected to be small and satisfy several requirements: (1) The average distance between each action encoding $\mathbf{v}_T^{(i)}$ and their prototype \mathbf{z}_i is small. (2) A cluster covers more action encoding (*i.e.*, P is large). To achieve this goal, we define ϕ as follows:

$$\phi = \frac{\sum_{i=1}^P \left\| \mathbf{v}_T^{(i)} - \mathbf{z}_i \right\|_2}{P \log(P + \alpha)}, \quad (8)$$

where α is a scaling parameter that avoids overwhelmingly large ϕ . On the other hand, ϕ serves as a punishing factor in the loss objective (see Sec. IV-B2) to generate more balanced clusters with similar tightness.

B. M-step

Next, we try to estimate $p(\mathbf{x}^{(i)}, \mathbf{z}_i | \theta)$. Due to the uniform probability over cluster centroids, we set $p(\mathbf{z}_i | \theta) = \frac{1}{K}$ and get:

$$\begin{aligned} p(\mathbf{x}^{(i)}, \mathbf{z}_i | \theta) &= p(\mathbf{x}^{(i)} | \mathbf{z}_i, \theta) p(\mathbf{z}_i | \theta) \\ &= \frac{1}{K} \cdot p(\mathbf{x}^{(i)} | \mathbf{z}_i, \theta). \end{aligned} \quad (9)$$

To calculate Eq. 9, we assume that the distribution for each action prototype is an isotropic Gaussian [18], which results in:

$$p(\mathbf{x}^{(i)} | \mathbf{z}_i, \theta) = \frac{\exp\left(\frac{-(\mathbf{v}_T^{(i)} - \mathbf{z}_s)^2}{2\sigma_s^2}\right)}{\sum_{k=1}^K \exp\left(\frac{-(\mathbf{v}_T^{(i)} - \mathbf{z}_k)^2}{2\sigma_k^2}\right)}, \quad (10)$$

where $\mathbf{v}_T^{(i)} \in \mathbf{z}_s$. Suppose ℓ_2 -normalization is applied to $\mathbf{v}_T^{(i)}$ and \mathbf{z}_i , then we have $(\mathbf{v}_T^{(i)} - \mathbf{z}_i)^2 = 2 - 2\mathbf{v}_T^{(i)} \cdot \mathbf{z}_i$. On the basis of Eq. 5, 6, 7, 9, 10, the maximum likelihood estimation is referred to as:

$$\theta^* = \arg \min_{\theta} \sum_{i=1}^N -\log \frac{\exp(\mathbf{v}_T^{(i)} \cdot \mathbf{z}_s / \phi_s)}{\sum_{k=1}^K \exp(\mathbf{v}_T^{(i)} \cdot \mathbf{z}_k / \phi_k)}, \quad (11)$$

Note that Eq. 11 is a kind of contrastive loss (similar as InfoNCE [26]), which evaluates the affinity between the action encoding and its assigned prototype over the affinity between that action encoding and other prototypes.

Based on Eq. 11, we further introduce sequential reverse prediction and add the related MAE loss to help preserve low-level information that can regenerate the sequence. Thus we construct the overall objective, namely ProtoMAE (see Sec. IV-B2).

² σ denotes standard deviation of data distribution

1) *Reverse Prediction*: Instead of performing commonly-used plain sequential prediction (see Sec. III-A) for action representation learning, we propose reverse prediction as to learn more high-level information (*e.g.* movement order) that are meaningful to human perception. Hence, we expect our model is able to generate predicted sequence $\hat{\mathbf{x}} = (\hat{\mathbf{x}}_1, \dots, \hat{\mathbf{x}}_T)$ that get closer to $\bar{\mathbf{x}} = \{\bar{\mathbf{x}}_1, \dots, \bar{\mathbf{x}}_T\} = \{\mathbf{x}_T, \dots, \mathbf{x}_1\}$, where $\bar{\mathbf{x}}_t = \mathbf{x}_{T-t+1}$. Then the MAE loss for reverse prediction is defined as:

$$\mathcal{L}_R = \frac{1}{T} \frac{1}{J} \sum_{t=1}^T \sum_{j=1}^J |\bar{\mathbf{x}}_{t,j} - \hat{\mathbf{x}}_{t,j}|. \quad (12)$$

2) *ProtoMAE Loss*: To this end, we combine Eq. 12 and Eq. 11 to form a new loss objective named ProtoMAE, defined as:

$$\mathcal{L}_{\text{ProtoMAE}} = \sum_{i=1}^N \left(\sum_{t=1}^T |\bar{\mathbf{x}}_t - \hat{\mathbf{x}}_t| - \frac{1}{M} \sum_{m=1}^M \log \frac{\exp\left(\frac{\mathbf{v}_T^{(i)} \cdot \mathbf{z}_s^m}{\phi_s^m}\right)}{\sum_{k=1}^r \exp\left(\frac{\mathbf{v}_T^{(i)} \cdot \mathbf{z}_k^m}{\phi_k^m}\right)} \right), \quad (13)$$

which is to be minimized to simultaneously achieve sequential reverse prediction and cluster the action encoding with semantic similarity. Note that in Eq. 13 large ϕ denotes the action encoding are in a loose cluster and small ϕ means they are in a tight cluster. Large ϕ weakens the affinity between the action encoding and the prototype, which drives the encoder to pull the action encoding closer to the prototype. In contrast, small ϕ does not compromise much to the affinity mentioned above, which less encourages the action encoding approach the prototype. Hence, learning with ProtoMAE generates more balanced clusters with similar tightness [18]. Besides, since the K may be too large, we choose to sample r prototypes, where $r < K$. We also attempt to cluster action encoding M times with different number of clusters $K = \{k_m\}_{m=1}^M$ to provide more robust probability estimation of prototypes.

EM algorithm performs E-step and M-step alternately without supervision for a specific epochs. Then the quality of learned representations \mathbf{v}_T from the encoder are measured by linear evaluation protocol [44], where the learned representations are always kept frozen and a linear classifier is added on top of them for training and testing.

V. EXPERIMENTS

Dataset: Experiments are based on three large action datasets and we use their skeleton sequences. (1) **Northwestern-UCLA (N-UCLA) Multiview Action 3D** dataset [37] consists of 10 classes of actions where every action is acted by 10 subjects. Three Kinect cameras record the action simultaneously and yield 1494 action videos in total. We adopt the same evaluation setting as in [43] by using samples from the first two views for training and the other for testing. (2) **NTU RGB+D 60** (NTU 60) dataset [30] is popular for skeleton based action recognition due to its variety of actions (60 classes) and its large scale (56578 samples). We follow the provided evaluation protocol: (a) Cross-Subject (C-Sub) setting that separates 40091 samples into training set

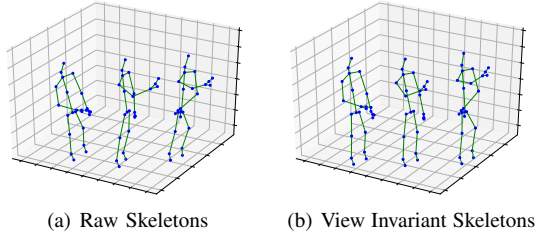


Fig. 3.

and the rest for testing set by different persons. (b) Cross-View (C-View) setting that covers 37646 samples captured by one camera for training and samples from the other camera are for testing. (3) **NTU RGB+D 120** (NTU 120) dataset [21] is NTU 60 based extension, whose scale is up to 120 classes of actions, 106 participants, and 113945 sequences in total. Similar as NTU 60, two validation protocols should be followed: (a) Cross-Subject (C-Sub) and (b) Cross-Setup (C-Set). In C-Sub, 63026 samples performed by 53 persons are for training and the others are for testing. In C-Set, all 32 setups are separated as a half for training and the other half for testing.

A. Configuration Details

Pre-processing: To overcome the orientation misalignment of skeleton movements shown in Fig. 3(a), we transform the raw data into a view-invariant coordinate system [16] as illustrated in Fig. 3(b). The transformed joint coordinates are then given by:

$$\mathbf{x}_{t,j} = \mathbf{R}^{-1}(\mathbf{x}_{t,j} - \mathbf{o}_R), \forall j \in J, \forall t \in T \quad (14)$$

where $\mathbf{x}_{t,j} \in \mathbb{R}^{3 \times 1}$. The rotation \mathbf{R} and the origin of rotation \mathbf{o}_R are determined by:

$$\mathbf{R} = \begin{bmatrix} \mathbf{u}_1 & \hat{\mathbf{u}}_2 & \mathbf{u}_1 \times \hat{\mathbf{u}}_2 \\ \|\mathbf{u}_1\| & \|\hat{\mathbf{u}}_2\| & \|\mathbf{u}_1 \times \hat{\mathbf{u}}_2\| \end{bmatrix}, \mathbf{o}_R = x_{1,\text{root}}, \quad (15)$$

where $\mathbf{u}_1 = x_{1,\text{spine}} - x_{1,\text{root}}$ denotes the vector vertical to the floor and $\hat{\mathbf{u}}_2 = \frac{\mathbf{u}_2 - \text{Proj}_{\mathbf{u}_1}(\mathbf{u}_2)}{\|\mathbf{u}_2 - \text{Proj}_{\mathbf{u}_1}(\mathbf{u}_2)\|}$ where $\mathbf{u}_2 = x_{1,\text{hip left}} - x_{1,\text{hip right}}$ denotes the difference vector between the left and right hip joints at the initial time step of each sample. $\text{Proj}_{\mathbf{u}_1}(\mathbf{u}_2)$ represents the vector projection of \mathbf{u}_2 onto \mathbf{u}_1 . \times is the cross product and $x_{1,\text{root}}$ is the spine base joint at the initial frame. The sequence length is fixed at 50 and we pad zeros if the sample is less than the fixed length.

PCRPs are based on the encoder-decoder structure of [34] with fixed weights for the decoder, but we replace Bi-GRU stated in [34] with the Uni-GRU for the encoder. We pre-train PCRPs for 50 epochs on the N-UCLA dataset and for 10 epochs on the NTU 60/120 dataset. The learning rate is 0.001 in pre-training stage. In the linear evaluation, we fix the encoder and train the linear classifier by 50 epochs on the N-UCLA dataset and by 30 epochs on the NTU 60/120 dataset. The learning rate is 0.01 in evaluation stage. Adam is applied for model optimization.

TABLE I
COMPARISON WITH PRIOR METHODS ON N-UCLA DATASET. “*” REPRESENTS DEPTH IMAGE BASED METHODS. BOLD NUMBERS REFER TO THE BEST PERFORMERS.

Id	Method	Acc (%)
Hand-Crafted Methods		
1	Lie Group [35]	74.2
2	Actionlet Ens [36]	76.0
Supervised Methods		
3	HBRNN-L [8]	78.5
Unsupervised Methods		
4	AS-CAL [29]	35.6
5	*Luo <i>et al.</i> [22]	50.7
6	*Li <i>et al.</i> [17]	62.5
7	LongT GAN [44]	74.3
8	MS ² L [20]	76.8
9	P&C FW [34]	83.3
10	PCRPs (Ours)	87.0

B. Performance Comparison

We compare our PCRPs with previous relevant unsupervised learning methods, supervised methods, and hand-crafted methods on three large datasets including N-UCLA dataset, NTU 60 dataset, and NTU 120 dataset. The performance comparisons are shown in Table I, II, III. For an unsupervised learning method P&C FW [34], we implement it on linear evaluation protocol instead of KNN evaluation, and also rid the auto-encoder part to be efficient in pre-training but not compromising much the performance.

1) *Comparison with Unsupervised Methods:* As shown in Table I on N-UCLA dataset, the proposed PCRPs shows 3.7-24.5% margin over the state-of-the-art unsupervised methods (Id = 6, 7, 8, 9), which are also based on the encoder-decoder structure to learn action representation. Although they possess cross-view decoding [17], additional adversarial training strategies [44], decoder-weakening mechanism [34] or multi-task learning [20], they just aim at plain sequential prediction in order and do not consider high-level semantic information learning. In contrast, the proposed PCRPs is able to simultaneously learn semantic similarity between sequences and enhance action representation learning via reverse prediction. In particular, our method achieves over 10% improvement than Li *et al.* (Id = 6) that focus on view-invariant action representation learning, which validates the superior robustness of our method to viewpoint variations. On the other hand, our approach takes skeleton sequences as inputs that are smaller sized than depth images, but it still significantly outperforms depth-image based methods (Id = 5, 6). Above advantages of our approach are also similarly shown on NTU 60 dataset (see Table II) and NTU 120 dataset (see Table III). These comparison results do show the effectiveness and efficacy of the proposed PCRPs.

Since our work is based on P&C FW [34], we make further comparison of our PCRPs with P&C FW on pre-training loss curves and evaluation accuracy curves. In Fig. 4(a) on N-UCLA dataset, we observe that PCRPs shows increasing margin than P&C FW as epoch goes on. When it comes to larger scale datasets, *i.e.*, NTU 60/120 dataset (see Fig. 4(b)-4(e)), the proposed work shows great superior over P&C FW that PCRPs keeps high evaluation accuracy from the beginning while P&C FW’s accuracy grows increasingly. We here argue

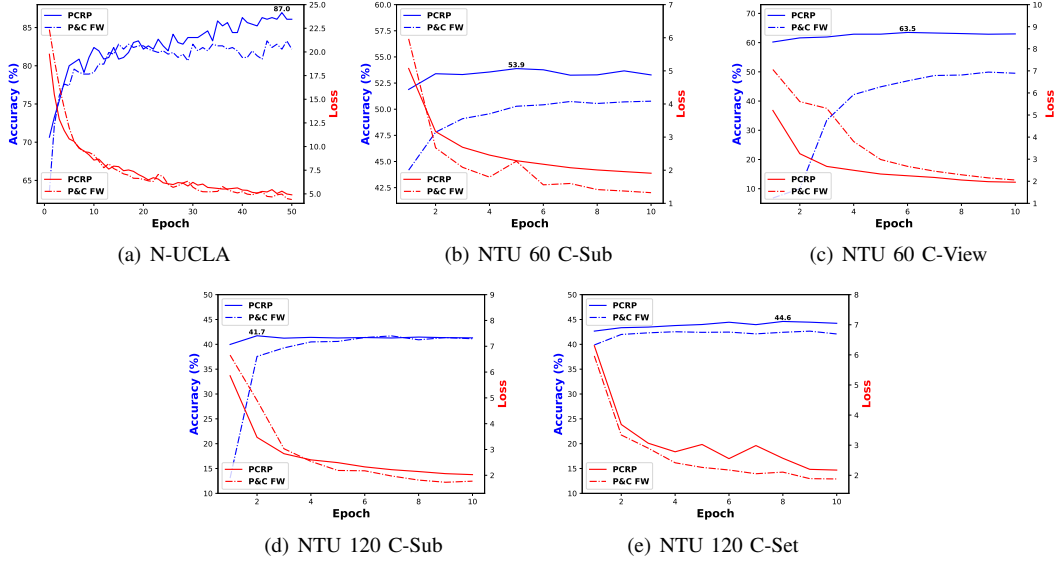


Fig. 4. Pre-training loss curves (red) and linear evaluation accuracy curves (blue) for three datasets.

TABLE II
COMPARISON WITH PRIOR METHODS ON NTU 60 DATASET. BOLD NUMBERS REFER TO THE BEST UNSUPERVISED PERFORMERS.

Id	Method	C-View Acc (%)	C-Sub Acc (%)
Hand-Crafted Methods			
1	*HON4D [25]	7.3	30.6
2	*Super Normal Vector [41]	13.6	31.8
3	*HOG ² [27]	22.3	32.2
4	Skeletal Quads [9]	41.4	38.6
5	Lie Group [35]	52.8	50.1
Supervised Methods			
6	HBRNN [8]	64.0	59.1
7	Deep RNN [30]	64.1	56.3
Unsupervised Methods			
8	*Shuffle&Learn [23]	40.9	46.2
9	*Luo <i>et al.</i> [22]	53.2	61.4
10	*Li <i>et al.</i> [17]	53.9	60.8
11	LongT GAN [44]	48.1	39.1
12	P&C FW [34]	44.3	50.8
13	MS ² L [20]	-	52.6
14	PCR P (Ours)	63.5	53.9

TABLE III
COMPARISON WITH SUPERVISED AND UNSUPERVISED METHODS ON NTU 120 DATASET. BOLD NUMBERS DENOTE THE BEST PERFORMERS.

Id	Method	C-Set Acc (%)	C-Sub Acc (%)
Supervised Methods			
1	Part-Aware LSTM [30]	26.3	25.5
2	Soft RNN [13]	44.9	36.3
Unsupervised Methods			
3	P&C FW [34]	42.7	41.7
4	PCR P (Ours)	45.1	41.7

that excellent unsupervised learning methods should be of high efficiency that they do not require too many pre-training epochs to achieve high evaluation accuracy, and they are supposed to maintain it as the epoch increases. From this point, our method indeed performs better than P&C FW. We plot confusion matrix results in Fig. 5

2) *Comparison with Hand-Crafted and Supervised Methods*: The proposed PCR P significantly surpasses several hand-crafted methods (Id = 1-2 in Table I) on the N-UCLA dataset

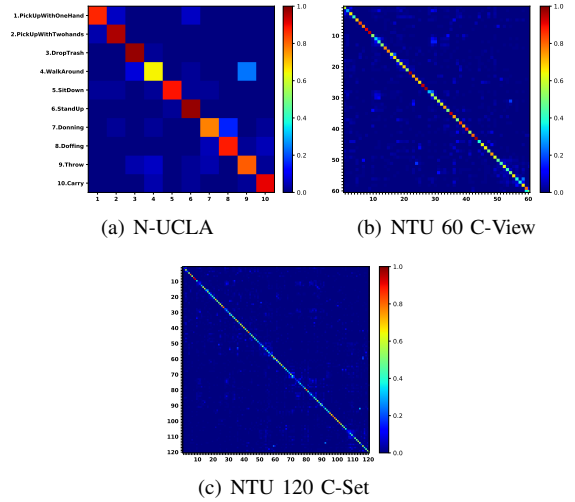


Fig. 5. Confusion Matrix

and (Id = 1-5 in Table II) on the NTU 60 dataset. For instance in Table II, PCR P shows better results than Skeletal Quads (Id = 4) and Lie group (Id = 5) by at least 10.7% on the C-View protocol and 3.8% on the C-Sub protocol. In addition, the proposed work is competitive or superior compared with some prior supervised methods on three datasets: (1) For the N-UCLA dataset in Table I, the proposed work has 6.5% margin better than HBRNN (Id = 3). (2) For the NTU 60 dataset in Table II, our method shows comparable results with Deep RNN (Id = 7). (3) For the NTU 120 dataset in Table III, our proposed approach presents advantage over Part-Aware LSTM (Id = 1) and Soft RNN (Id = 2) by 0.2-18.8% on different evaluation settings.

C. Ablation Study

In this section, we conduct extensive ablation experiments on three datasets mentioned above to provide solid validation

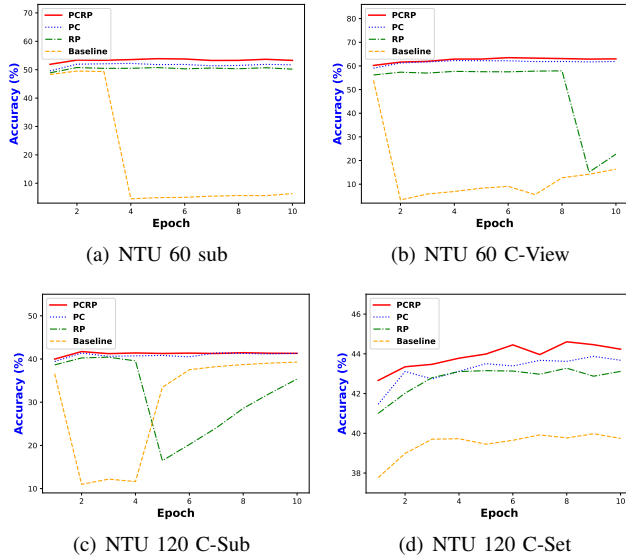


Fig. 6. Linear evaluation accuracy curves of PCRCP, PC, RP, and baseline on NTU 60/120 dataset.

of our proposed work.

1) *Analysis of PC and RP*: In this part, we explore the role of prototypical contrast (PC) and reverse prediction (RP). The baseline is P&C FW [34] with Uni-GRU encoder instead of Bi-GRU stated in [34]. When the experiment is involved in PC, we run $M = 3$ times clustering with different cluster number (see Eq. 13).

In Table IV(a) for the N-UCLA dataset, compared with the baseline (Id = 1), RP (Id = 2) presents 0.9% improvement, which validates the effectiveness of RP in our framework. This effectiveness can also be observed from the comparison between (Id = 3) and (Id = 4). For the effective function of PC, the item (Id = 3) runs 3 times clustering with 40, 70, 100 clusters respectively and it shows superior performance over the baseline (Id = 1) by 2.5%. Besides, the item (Id = 4) also shows 2.8% margin higher than (Id = 2). Combing PC and RP, the final model (Id = 4) achieves the best result. In the larger datasets such as NTU 60/120 dataset, the effectiveness of PC and RP can also be demonstrated and shown in Table IV(b) and Table IV(c).

Furthermore, we plot evaluation accuracy curves of PCRCP, PC, RP, and baseline on NTU 60/120 dataset. As shown in Table 6(a)-6(d), our approach PCRCP (red line) is able to obtain high evaluation accuracy at beginning and then maintain it as the pre-training goes on, which shows its powerful and robust action representation learning.

2) *Effects of Various Number of Clusters*: To understand the effects of M times running with different cluster number, we conduct ablation experiments on the N-UCLA dataset, the NTU 60 dataset in C-View setting, and the NTU 120 dataset in C-Set setting. As shown in Table V(a), $M = 1$ with 70 clusters for PC (Id = 2) obtains 87.0%, which outperforms $M = 3$ times running for PC (Id = 4-5). Likewise, Table V(c) has similar observation. In Table V(b), $M = 3$ with 90, 120, 150 (Id = 5) achieves 63.5%, the highest score among (Id = 1-6). Along this line, we can understand running larger M

TABLE IV
ABLATION EXPERIMENTS OF PCRCP.

(a) N-UCLA				(b) NTU 60				
Id	RP	Clusters	Acc (%)	Id	RP	Clusters	C-View Acc (%)	C-Sub Acc (%)
1	×	×	82.6	1	×	×	53.9	49.5
2	✓	×	83.5	2	✓	×	57.9	50.8
3	×	40,70,100	86.1	3	×	90,120,150	62.3	52.2
4	✓	40,70,100	86.3	4	✓	90,120,150	63.5	53.9

(c) NTU 120

Id	RP	Clusters	C-Set Acc (%)	C-Sub Acc (%)
1	×	×	40.0	39.3
2	✓	×	43.3	40.4
3	×	150,180,210	43.9	41.4
4	✓	150,180,210	44.6	41.7

TABLE V
ABLATION EXPERIMENTS OF M OF EQ. 13

(a) N-UCLA				(b) NTU 60 C-View			
Id	M	Clusters	Acc (%)	Id	M	Clusters	Acc (%)
1	1	40	86.5	1	1	90	62.5
2	1	70	87.0	2	1	120	62.8
3	1	100	85.4	3	1	150	62.9
4	3	30,60,90	86.5	4	3	80,110,140	62.6
5	3	40,70,100	86.3	5	3	90,120,150	63.5
6	3	50,80,110	86.3	6	3	100,130,160	62.8

(c) NTU 120 C-Set

Id	M	Clusters	Acc (%)
1	1	150	43.6
2	1	180	45.1
3	1	210	44.1
4	3	150,180,210	44.6
5	3	160,190,220	43.9
6	3	170,200,230	43.2

with different cluster number does not necessarily guarantee better representation.

VI. CONCLUSION

This paper presents a novel framework named prototypical contrast and reverse prediction (PCRCP) for skeleton-based action recognition. In the view of EM algorithm, PCRCP alternately performs E-step as generating action prototypes by clustering action encoding from the encoder, and M-step as updating the encoder by contracting the distribution around the prototypes and simultaneously predicting sequences in reverse order. Experiments on three large datasets show that our work can learn distinct action representations and surpass previous unsupervised approaches.

REFERENCES

- [1] Vijay Badrinarayanan, Alex Kendall, and Roberto Cipolla. Segnet: A deep convolutional encoder-decoder architecture for image segmentation. *IEEE transactions on pattern analysis and machine intelligence*, 39(12):2481–2495, 2017. 1
- [2] Bharat Lal Bhatnagar, Suriya Singh, Chetan Arora, CV Jawahar, and KCIS CVIT. Unsupervised learning of deep feature representation for clustering egocentric actions. In *IJCAI*, pages 1447–1453, 2017. 2
- [3] Mathilde Caron, Ishan Misra, Julien Mairal, Priya Goyal, Piotr Bojanowski, and Armand Joulin. Unsupervised learning of visual features by contrasting cluster assignments. *arXiv preprint arXiv:2006.09882*, 2020. 2
- [4] Ting Chen, Simon Kornblith, Mohammad Norouzi, and Geoffrey Hinton. A simple framework for contrastive learning of visual representations. *ICML2020*, 2020. 2

- [5] Ke Cheng, Yifan Zhang, Xiangyu He, Weihang Chen, Jian Cheng, and Hanqing Lu. Skeleton-based action recognition with shift graph convolutional network. In *CVPR*, June 2020. 1, 2
- [6] Arthur P Dempster, Nan M Laird, and Donald B Rubin. Maximum likelihood from incomplete data via the em algorithm. *Journal of the Royal Statistical Society: Series B (Methodological)*, 39(1):1–22, 1977. 1
- [7] Laurence Devillers, Laurence Vidrascu, and Lori Lamel. Challenges in real-life emotion annotation and machine learning based detection. *Neural Networks*, 18(4):407–422, 2005. 1
- [8] Yong Du, Wei Wang, and Liang Wang. Hierarchical recurrent neural network for skeleton based action recognition. In *CVPR*, pages 1110–1118, 2015. 5, 6
- [9] Georgios Evangelidis, Gurbir Singh, and Radu Horaud. Skeletal quads: Human action recognition using joint quadruples. In *ICPR*, pages 4513–4518. IEEE, 2014. 6
- [10] Michael Gutmann and Aapo Hyvärinen. Noise-contrastive estimation: A new estimation principle for unnormalized statistical models. In *International Conference on Artificial Intelligence and Statistics*, pages 297–304, 2010. 2
- [11] Raia Hadsell, Sumit Chopra, and Yann LeCun. Dimensionality reduction by learning an invariant mapping. In *CVPR*, volume 2, pages 1735–1742. IEEE, 2006. 2
- [12] Kaiming He, Haoqi Fan, Yuxin Wu, Saining Xie, and Ross Girshick. Momentum contrast for unsupervised visual representation learning. In *CVPR*, June 2020. 2
- [13] Jian-Fang Hu, Wei-Shi Zheng, Lianyang Ma, Gang Wang, Jian-Huang Lai, and Jianguo Zhang. Early action prediction by soft regression. *TPAMI*, 2018. 6
- [14] Simon Jones and Ling Shao. Unsupervised spectral dual assignment clustering of human actions in context. In *CVPR*, June 2014. 2
- [15] Tejas D Kulkarni, Ankush Gupta, Catalin Ionescu, Sebastian Borgeaud, Malcolm Reynolds, Andrew Zisserman, and Volodymyr Mnih. Unsupervised learning of object keypoints for perception and control. In *NeurIPS*, pages 10723–10733, 2019. 1
- [16] Inwoong Lee, Doyoung Kim, Seoungyoon Kang, and Sanghoon Lee. Ensemble deep learning for skeleton-based action recognition using temporal sliding lstm networks. In *Proceedings of the IEEE international conference on computer vision*, pages 1012–1020, 2017. 5
- [17] Junnan Li, Yongkang Wong, Qi Zhao, and Mohan Kankanhalli. Unsupervised learning of view-invariant action representations. In *NeurIPS*, pages 1254–1264, 2018. 5, 6
- [18] Junnan Li, Pan Zhou, Caiming Xiong, Richard Socher, and Steven CH Ho. Prototypical contrastive learning of unsupervised representations. *arXiv preprint arXiv:2005.04966*, 2020. 1, 2, 3, 4
- [19] Duohan Liang, Guoliang Fan, Guangfeng Lin, Wanjuan Chen, Xiaorong Pan, and Hong Zhu. Three-stream convolutional neural network with multi-task and ensemble learning for 3d action recognition. In *CVPR Workshops*, June 2019. 1, 2
- [20] Lilang Lin, Sijie Song, Wenhan Yang, and Jiaying Liu. Ms2l: Multi-task self-supervised learning for skeleton based action recognition. In *Proceedings of the 28th ACM International Conference on Multimedia*, pages 2490–2498, 2020. 1, 5, 6
- [21] Jun Liu, Amir Shahroudy, Mauricio Lisboa Perez, Gang Wang, Ling-Yu Duan, and Alex Kot Chichung. Ntu rgb+ d 120: A large-scale benchmark for 3d human activity understanding. *TPAMI*, 2019. 5
- [22] Zelun Luo, Boya Peng, De-An Huang, Alexandre Alahi, and Li Fei-Fei. Unsupervised learning of long-term motion dynamics for videos. In *CVPR*, pages 2203–2212, 2017. 1, 5, 6
- [23] Ishan Misra, C Lawrence Zitnick, and Martial Hebert. Shuffle and learn: unsupervised learning using temporal order verification. In *ECCV*, pages 527–544. Springer, 2016. 6
- [24] Thu Nguyen-Phuoc, Chuan Li, Lucas Theis, Christian Richardt, and Yong-Liang Yang. Hologan: Unsupervised learning of 3d representations from natural images. In *ICCV*, pages 7588–7597, 2019. 1
- [25] Eshed Ohn-Bar and Mohan M. Trivedi. Joint angles similarities and hog2 for action recognition. In *CVPR Workshops*, June 2013. 6
- [26] Aaron van den Oord, Yazhe Li, and Oriol Vinyals. Representation learning with contrastive predictive coding. *arXiv preprint arXiv:1807.03748*, 2018. 4
- [27] Omar Oreifej and Zicheng Liu. Hon4d: Histogram of oriented 4d normals for activity recognition from depth sequences. In *CVPR*, June 2013. 6
- [28] Bo Peng, Jianjun Lei, Huazhu Fu, Ling Shao, and Qingming Huang. A recursive constrained framework for unsupervised video action clustering. *IEEE Transactions on Industrial Informatics*, 16(1):555–565, 2019. 2
- [29] Haocong Rao, Shihao Xu, Xiping Hu, Jun Cheng, and Bin Hu. Augmented skeleton based contrastive action learning with momentum lstm for unsupervised action recognition, 2020. 1, 2, 5
- [30] Amir Shahroudy, Jun Liu, Tian-Tsong Ng, and Gang Wang. Ntu rgb+ d: A large scale dataset for 3d human activity analysis. In *CVPR*, pages 1010–1019, 2016. 4, 6
- [31] Lei Shi, Yifan Zhang, Jian Cheng, and Hanqing Lu. Skeleton-based action recognition with directed graph neural networks. In *CVPR*, June 2019. 2
- [32] Lei Shi, Yifan Zhang, Jian Cheng, and Hanqing Lu. Skeleton-based action recognition with multi-stream adaptive graph convolutional networks, 2019. 1
- [33] Chenyang Si, Wentao Chen, Wei Wang, Liang Wang, and Tieniu Tan. An attention enhanced graph convolutional lstm network for skeleton-based action recognition. In *CVPR*, pages 1227–1236, 2019. 1
- [34] Kun Su, Xiulong Liu, and Eli Shlizerman. Predict & cluster: Unsupervised skeleton based action recognition. In *CVPR*, pages 9631–9640, 2020. 1, 2, 5, 6, 7
- [35] Raviteja Vemulapalli, Felipe Arrate, and Rama Chellappa. Human action recognition by representing 3d skeletons as points in a lie group. In *CVPR*, pages 588–595, 2014. 5, 6
- [36] Jiang Wang, Zicheng Liu, Ying Wu, and Junsong Yuan. Learning actionlet ensemble for 3d human action recognition. *TPAMI*, 36(5):914–927, 2013. 5
- [37] Jiang Wang, Xiaohan Nie, Yin Xia, Ying Wu, and Song-Chun Zhu. Cross-view action modeling, learning and recognition. In *CVPR*, June 2014. 4
- [38] Xin-Jing Wang, Lei Zhang, Feng Jing, and Wei-Ying Ma. Annosearch: Image auto-annotation by search. In *CVPR*, volume 2, pages 1483–1490. IEEE, 2006. 1
- [39] Zhirong Wu, Yuanjun Xiong, Stella X Yu, and Dahua Lin. Unsupervised feature learning via non-parametric instance discrimination. In *CVPR*, pages 3733–3742, 2018. 2
- [40] Sijie Yan, Yuanjun Xiong, and Dahua Lin. Spatial temporal graph convolutional networks for skeleton-based action recognition. In *AAAI*, 2018. 1
- [41] Xiaodong Yang and YingLi Tian. Super normal vector for activity recognition using depth sequences. In *CVPR*, June 2014. 6
- [42] Pengfei Zhang, Cuiling Lan, Junliang Xing, Wenjun Zeng, Jianru Xue, and Nanning Zheng. View adaptive recurrent neural networks for high performance human action recognition from skeleton data. In *ICCV*, pages 2117–2126, 2017. 1
- [43] Pengfei Zhang, Jianru Xue, Cuiling Lan, Wenjun Zeng, Zhanning Gao, and Nanning Zheng. Eleatt-rnn: Adding attentiveness to neurons in recurrent neural networks. *TIP*, 29:1061–1073, 2020. 4
- [44] Nenggan Zheng, Jun Wen, Risheng Liu, Liangqu Long, Jianhua Dai, and Zhefeng Gong. Unsupervised representation learning with long-term dynamics for skeleton based action recognition. In *AAAI*, 2018. 1, 2, 4, 5, 6
- [45] Chengxu Zhuang, Alex Lin Zhai, and Daniel Yamins. Local aggregation for unsupervised learning of visual embeddings. In *ICCV*, pages 6002–6012, 2019. 2